

Box-based and Laguerre-based convergent close-coupling calculations of electron–helium ionization

I Bray¹, K Bartschat^{1,3}, D V Fursa² and A T Stelbovics¹

¹ Centre for Atomic, Molecular and Surface Physics, Physics and Energy Studies, Murdoch University, Perth 6150, Australia

² SoCPES, Flinders University, GPO Box 2100, Adelaide 5001, Australia

E-mail: I.Bray@murdoch.edu.au

Received 11 June 2003

Published 23 July 2003

Online at stacks.iop.org/JPhysB/36/3425

Abstract

We apply a new implementation of the convergent close-coupling (CCC) method to electron–helium scattering. The target states are obtained from one-electron He⁺ box-based eigenstates rather than the usual Laguerre-based orbitals. The utility of the new method is demonstrated for 50 eV electron-impact ionization of helium with three different energy sharings between the two outgoing electrons. Excellent agreement is found between previous and new CCC predictions, and also with experimental data.

1. Introduction

In recent years there has been considerable progress in the related fields of electron-impact ionization and double photoionization of light atomic targets (see, for example, Briggs and Schmidt 2000 and Bray *et al* 2002 for recent reviews). This progress has predominantly come from computationally intensive techniques that attempt an accurate numerical evaluation of the total wavefunction. The exterior complex scaling (ECS) approach (Rescigno *et al* 1999, Baertschy *et al* 2001) was the first method to yield accurate triple-differential cross sections (TDCS) for e–H ionization, and the convergent close-coupling (CCC) method followed soon after Bray (2002). Whereas the ECS technique has thus far been applied predominantly to model problems and the physical e–H collision system, the CCC method has been used for electron and photon collisions with various atoms and ions (Bray *et al* 2002), as well as for positron collisions with positronium formation included (Kadyrov and Bray 2002).

The present paper deals with the problem of e–He ionization. Only recently, the CCC approach to such problems has been understood (Bray *et al* 2001). Earlier CCC calculations generally yielded good agreement with experimental angular distributions but uncertain

³ Permanent address: Department of Physics and Astronomy, Drake University, Des Moines, IA 50311, USA.

magnitudes. In cases of equal energy-sharing kinematics, for example, the cross sections were a factor of 2 or so too low (Bray *et al* 1997, 1998, Rioual *et al* 1998), and substantial magnitude differences were also found for asymmetric energy sharing (Röder *et al* 1997). The latter study of double-differential cross sections (DDCSs) was recently re-examined, and a much more satisfactory agreement with experimental data was obtained (Bray *et al* 2003b).

With the magnitude issues effectively resolved (Bray *et al* 2001), we now reconsider the few cases, in which the CCC method was previously shown to work particularly poorly, not just for the magnitude but also for the shape of the angular distributions. One such case is the electron-impact ionization of helium at an incident energy of 50 eV. Three different energy sharings between the two outgoing electrons were measured, and the one where the slow electron had 10 eV yielded particularly poor results (Röder *et al* 1996a). We also take this opportunity to apply a recently introduced alternative version of the CCC method to this problem. In this new formulation, the Laguerre-based orbitals used in the original CCC method are replaced by box-based orbitals to generate the physical and pseudo target states. This approach has been shown to work well at very low impact energies for e–H ionization (Bray *et al* 2003a). We will show below that it works equally well for the helium target and at a considerably larger energy.

2. Structure calculations

The details of the CCC approach to e–He collisions have been given by Fursa and Bray (1995). These are just as relevant in the boxed-based CCC-B method, except that the orthonormal one-electron orbitals are obtained by generating a set of He⁺ eigenstates in a box of fixed radius R_0 , with the boundary conditions for the orbitals being zero at $r = 0$ and $r \geq R_0$. This generates a natural eigenstate discretization of the continuum, yielding true $Z = 2$ Coulomb waves for those momenta k_n with a node at R_0 . These orbitals are then used to construct two-electron configurations, and the physical and pseudo states are generated by diagonalizing the neutral-helium target Hamiltonian.

Note that the number of physical discrete eigenstates is controlled by the box radius. Physical states will effectively fit in the box, while pseudo states will not. Apart from the exponential fall-off of the Laguerre-based orbitals, compared to the sudden fall-off of the box-based orbitals, a major difference between the two sets of orbitals is the energy spectrum. The latter set yields an almost linear discretization in the positive momenta (the subsequent k_n values will differ by approximately π/R_0), whereas the former has them growing much more rapidly (see, for example, Bray *et al* 2003a). The corresponding two-electron target spectra, as chosen in the two CCC calculations performed here for 50 eV e–He ionization, are shown in figure 1. Note that both yield much the same negative-energy discrete and low-positive-energy spectra. With increasing energy, however, the box-based states provide a much denser discretization of the continuum.

Both calculations use the frozen-core approximation, in which one of the target electrons is described by the exact He⁺ 1s orbital. The maximum target-space orbital angular momentum was set at $l_{\max} = 4$. In the Laguerre-based CCC-L calculation, we took the first $25 - l$ orbitals for each l , as obtained from diagonalizing the He⁺ Hamiltonian in a Laguerre basis with $N_l = 29 - l$ and $\lambda = 2.2$. The four highest energy orbitals could be dropped because they do not significantly contribute to the convergence of the ground-state description and would generate closed helium states with energies much in excess of 25.4 eV, which is the total excess energy E shared by the two outgoing electrons. In the CCC-L calculation presented, the total number of coupled states was 229.

The structure considerations in the CCC-B calculation are quite different. The He⁺ orbitals were obtained by setting $R_0 = 50 a_0$ and taking the first $N_l = 30 - l$ of them to form the two-

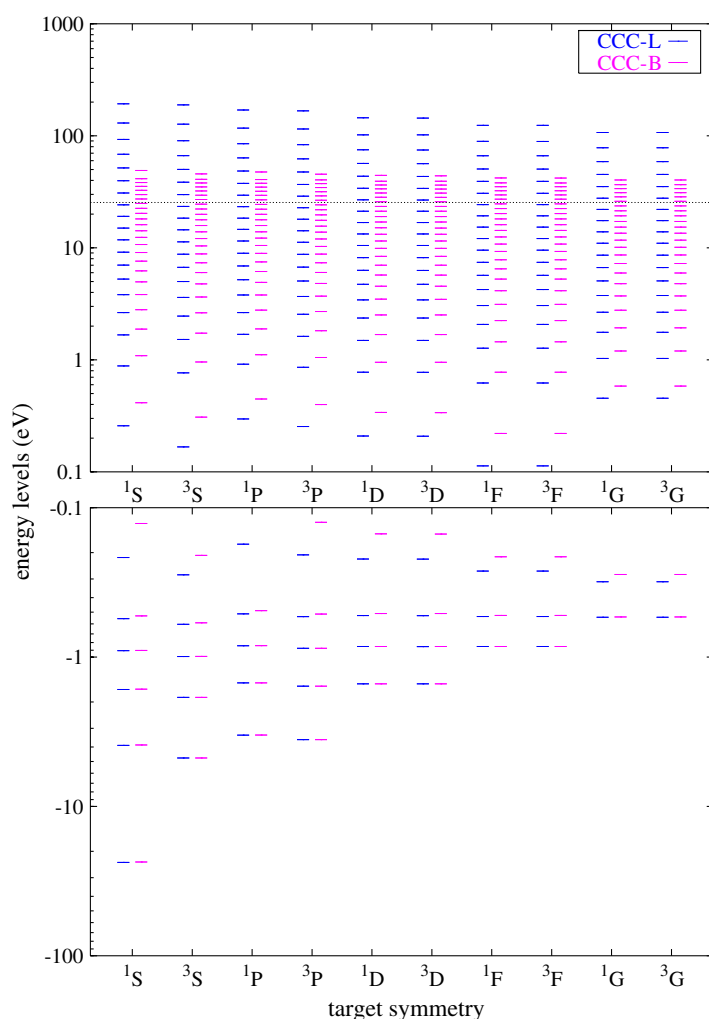


Figure 1. Energy levels of the 50 eV Laguerre-based (CCC-L, left column for each symmetry) and box-based (CCC-B, right column) calculations. The total energy of 25.4 eV is indicated by the black line.

(This figure is in colour only in the electronic version)

electron configurations and then diagonalize the neutral-helium target Hamiltonian. In this case a balance needs to be struck between choosing R_0 as large as possible while including as many He^+ orbitals as computationally tractable. Using this basis, we are somewhat constrained by the need for a sufficient number of high-energy orbitals to obtain convergence in the description of the ground state. Using $N_l = 30 - l$ already leads to 279 states, even though the high energies in the spectrum are substantially lower than those of the corresponding CCC-L states, due to the fine discretization of the continuum. Even with the choices given above, the frozen-core helium ground state in the CCC-B model is not quite converged. The CCC-L model reproduces the known error of about 0.84 eV in the frozen-core approximation of the helium ionization energy, while the corresponding error in the CCC-B model remained at around 1 eV.

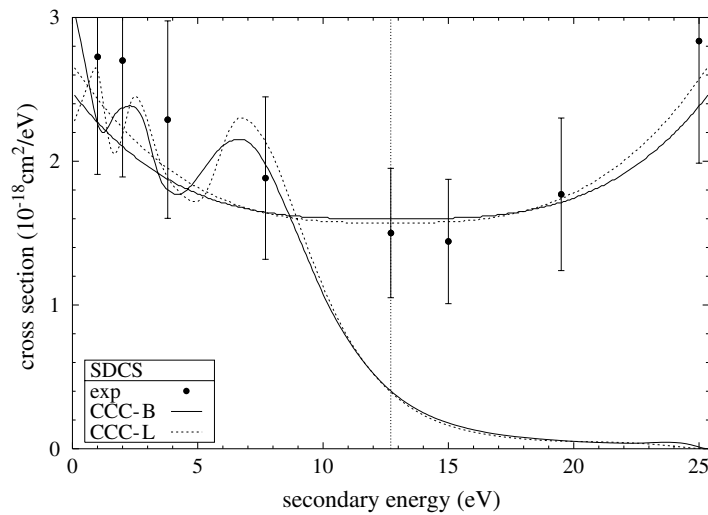


Figure 2. Single-differential cross sections predicted by the two CCC calculations for 50 eV e–He ionization. The oscillatory curves correspond to the raw results, while the curves that are symmetric around equal energy sharing at 12.7 eV are integral-preserving (on the [0,12.7] eV energy range) estimates with the midpoint taken as four times the raw result. The experimental data are taken from Röder *et al* (1997), marginally modified by Bray *et al* (2003b).

3. Results and discussion

It is only the pseudo-target structure that differentiates the CCC-B and CCC-L calculations. The evaluation of 50 eV e–He scattering proceeds in the same manner as before (Fursa and Bray 1995). Upon generation of the T -matrix elements the ionization amplitudes are defined in the way specified by Bray and Fursa (1996) and elaborated further by Bray *et al* (2001).

We begin our test of the two CCC calculations by comparing their predictions for the total ionization cross sections (TICS). These are obtained directly as sums of the excitation cross sections for all positive-energy states. The experimental (Montague *et al* 1984, Shah *et al* 1988), CCC-B and CCC-L values (in 10^{-17} cm²) are 2.37 ± 0.11 , 2.30 and 2.35, respectively.

A more detailed set of ionization data are provided by the single-differential (with respect to the energy loss) cross section (SDCS), which may also be obtained directly from the positive-energy integrated cross sections (Bray and Fursa 1995). The results are exhibited in figure 2. The raw CCC results fall off rapidly to zero past $E/2$, but the integral from 0 to E yields the TICS. Oscillations on the secondary energy range $[0, E/2]$ are expected (Bray *et al* 2001), but the similarity of the oscillations might at first be surprising in light of the rather different discretizations seen in figure 1. As the oscillations are due to a Fourier-like expansion of a step function, one might have expected that a denser discretization would yield more oscillatory results, but this is not the case. The quality of the step-function reproduction depends on the effective R_0 in the calculation, with the larger R_0 yielding more oscillations and a sharper step, see for example Scott *et al* (2002) and Bartschat *et al* (2002). The two symmetric (about $E/2$) curves are integral-preserving estimates, whose mid-point is obtained as four times the raw result (Bray *et al* 2001). The similarity of the two curves is quite encouraging. These estimates are used to rescale the subsequent angle-differential cross sections. This ensures consistency, upon angular integration, with the estimated SDCSs.

The DDCSs are given in figure 3 and are compared with the absolute experimental data of Röder *et al* (1997), subject to the minor modifications of Bray *et al* (2003b). We see

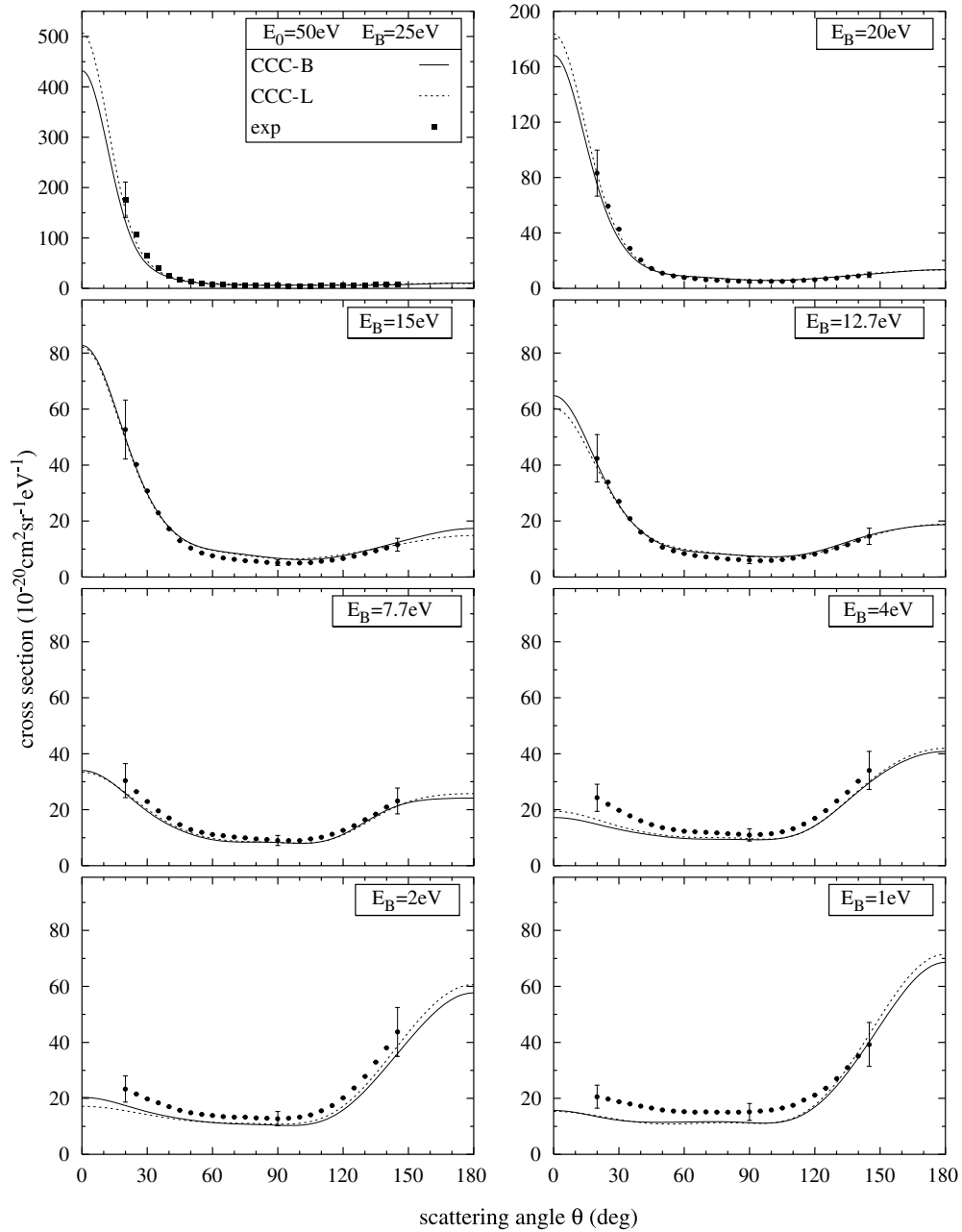


Figure 3. Double-differential cross sections predicted in the two CCC models for 50 eV e-He ionization. The experimental data are taken from Röder *et al* (1997), subject to the minor reanalysis of Bray *et al* (2003b).

a remarkable similarity between the two sets of theoretical predictions and also excellent agreement with the experimental data. Note that the CCC ionization amplitudes are initially available only at the energies given in figure 1, and thus the values at the experimentally

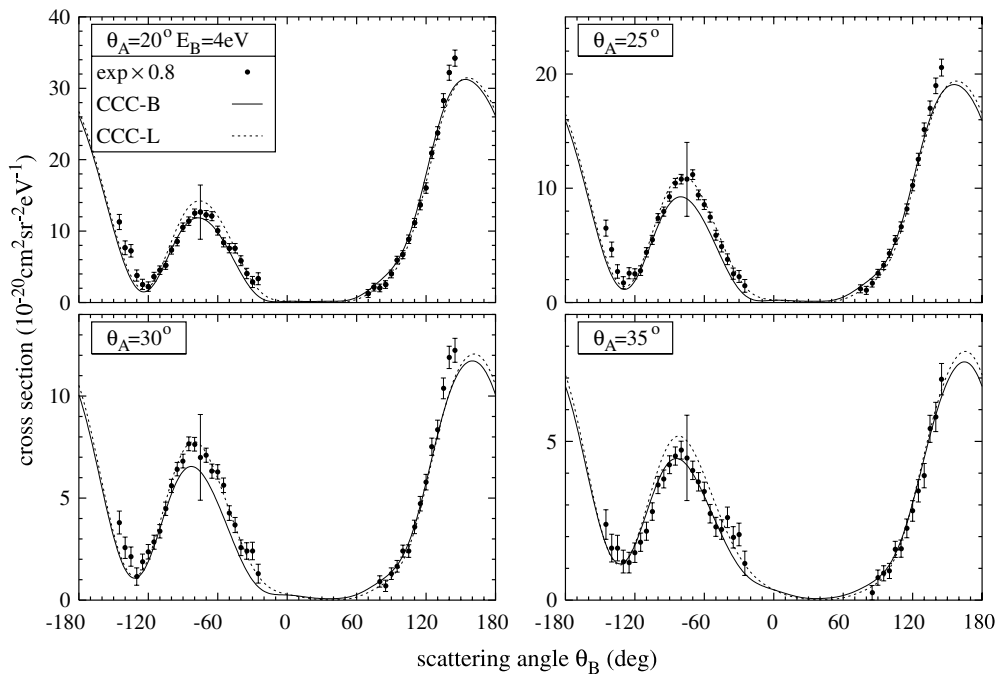


Figure 4. Coplanar TDCS predicted in the two CCC models for 50 eV e–He ionization, with the 4 eV electron detected at θ_B and the 21.4 eV electron detected at θ_A . The absolute experimental data are taken from Röder *et al* (1996b).

measured energies E_B are obtained by interpolation. Both methods have enough states to yield accurate interpolation of the underlying complex values.

We now consider the TDCS at the three measured energy sharings. The case with the slow-electron energy of $E_B = 4$ eV is presented in figure 4. Four internormalized geometries were measured by Röder *et al* (1996a) and put on an absolute scale with an overall uncertainty of 30%, as indicated by the larger error bars. For a better visual fit to the theoretical predictions, we reduced the published experimental data by 20%. This reduction is not surprising, since the experimental SDCS at 4 eV is also about 20% higher than the theoretical value. Note that there is little need for rescaling the theoretical results here, as the estimate and the raw result are much the same. We see excellent agreement between experiment and the two sets of theoretical predictions, as was the case earlier (Röder *et al* 1996a).

The other asymmetric energy-sharing case measured is for a slow-electron energy of 10 eV. This case provides for a particularly stringent test of CCC theory since it is close to, but not quite at, equal energy sharing. As can be seen from figure 2, the raw CCC result for the SDCS falls rapidly in this energy region, thus requiring substantial rescaling of the raw magnitudes. Note the early CCC calculations failed to reproduce these data sets in both shape and magnitude (Röder *et al* 1996a). The present calculations, however, exhibited in figure 5, show very good agreement between the two theoretical curves and the experimental data in both shape and magnitude, with only minor discrepancies remaining. The main reason for the improvement is the much denser discretization in the present CCC calculations.

Finally, we consider the case of equal energy sharing in figure 6. The only data available here are for the so-called ‘doubly symmetric geometry’, i.e. $E_A = E_B$ and $\theta_A = -\theta_B$. These experimental data, obtained by Rösel *et al* (1992), are relative and have been normalized to the

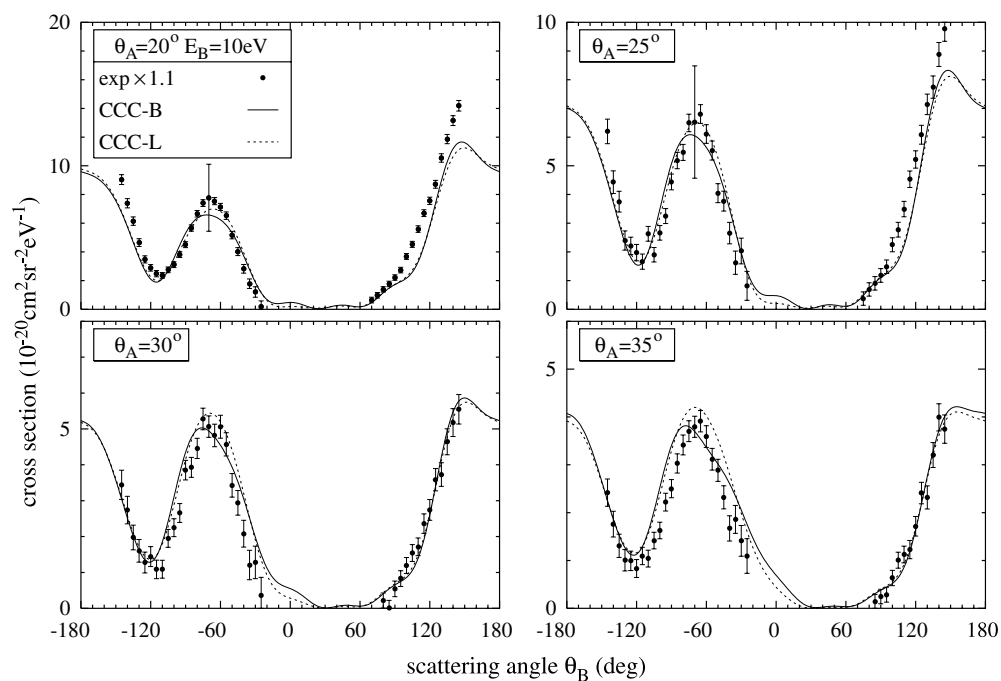


Figure 5. Same as figure 4, except that the slow electron has an energy of 10 eV while the fast electron has 15.4 eV.

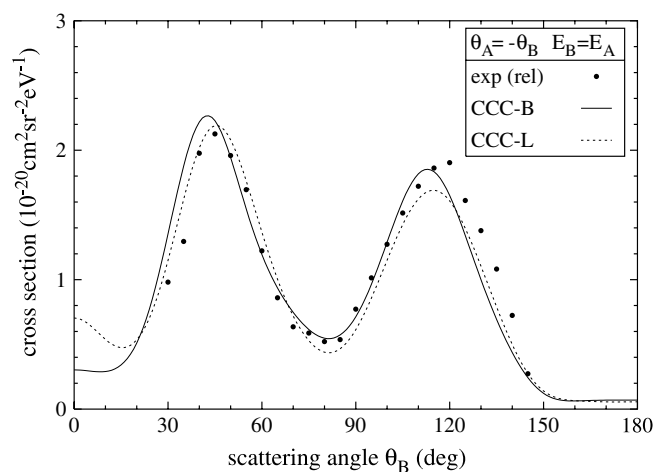


Figure 6. Doubly symmetric coplanar TDCS predicted in the two CCC models for 50 eV e-He ionization. The relative data of Rösel *et al* (1992) were normalized to the theoretical predictions for a good visual fit.

theory. While the shape agreement with the available experimental data are very satisfactory for both models, we note that the CCC-B calculation yields better near-zero cross sections for small angles. This is likely due to the denser discretization of the continuum, thereby allowing for a more accurate interpolation of the underlying amplitudes.

4. Summary and conclusions

We have applied a new variant of the CCC method to e–He scattering. It is based on one-electron orbitals that are solutions of the Coulomb problem within a box of radius R_0 . The positive-energy orbitals are the true continuum eigenstates which vanish at R_0 and are truncated to zero outside the box. In this respect they are very different from Laguerre-based orbitals which fall off exponentially beyond the last node. The good agreement between all predictions from the CCC-L and CCC-B calculations presented here suggests that the substantial differences in the tails of the orbitals occur at sufficiently large distances to have a nearly insignificant effect on the calculated ionization cross sections. Although the substantially denser discretization in the CCC-B method does not necessarily yield a better representation of the underlying step function in the SDCSs, it does assist in yielding greater accuracy in the interpolation of the complex amplitudes that are only known at the discrete energies of the continuum pseudo states. Another conceptual advantage of the CCC-B approach is the underlying simplicity of the formulation. Apart from the usual angular momentum considerations, convergence studies may be performed by simply increasing R_0 while keeping the additional states generated. Alternatively, the particularly dense discretization makes it difficult to include high-energy orbitals which are required for convergence in the description of the initial ground state.

Acknowledgments

This work was supported, in part, by the Australian Research Council and the United States National Science Foundation. Support of the Australian Research Council and the Merit Allocation Scheme on the National Facility of the Australian Partnership for Advanced Computing is gratefully acknowledged. KB would like to thank Murdoch University for the hospitality received during his visit sponsored by an international research exchange programme.

References

- Baertschy M, Rescigno T N and McCurdy C W 2001 *Phys. Rev. A* **64** 022709
- Bartschat K, Scott M P, Burke P G, Stitt T, Scott N S, Grum-Grzhimailo A N, Riordan S, Ver Steeg G and Strakhova S I 2002 *Phys. Rev. A* **65** 062715
- Bray I 2002 *Phys. Rev. Lett.* **89** 273201
- Bray I, Bartschat K and Stelbovics A T 2003a *Phys. Rev. A* **67** 060704(R)
- Bray I and Fursa D V 1995 *J. Phys. B: At. Mol. Opt. Phys.* **28** L435–41
- Bray I and Fursa D V 1996 *Phys. Rev. A* **54** 2991–3004
- Bray I, Fursa D V, Kheifets A S and Stelbovics A T 2002 *J. Phys. B: At. Mol. Opt. Phys.* **35** R117–46
- Bray I, Fursa D V, Röder J and Ehrhardt H 1997 *J. Phys. B: At. Mol. Opt. Phys.* **30** L101–8
- Bray I, Fursa D V, Röder J and Ehrhardt H 1998 *Phys. Rev. A* **57** R3161–4
- Bray I, Fursa D V and Stelbovics A T 2001 *Phys. Rev. A* **63** 040702(R)
- Bray I, Fursa D V and Stelbovics A T 2003b *J. Phys. B: At. Mol. Opt. Phys.* **36** 2211–27
- Briggs J and Schmidt V 2000 *J. Phys. B: At. Mol. Opt. Phys.* **33** R1–48
- Fursa D V and Bray I 1995 *Phys. Rev. A* **52** 1279–98
- Kadyrov A S and Bray I 2002 *Phys. Rev. A* **66** 012710
- Montague R G, Harrison M F A and Smith A C H 1984 *J. Phys. B: At. Mol. Phys.* **17** 3295–310
- Rescigno T N, Baertschy M, Isaacs W A and McCurdy C W 1999 *Science* **286** 2474–9
- Rioual S, Röder J, Rouvellou B, Ehrhardt H, Pochat A, Bray I and Fursa D V 1998 *J. Phys. B: At. Mol. Opt. Phys.* **31** 3117–27
- Röder J, Ehrhardt H, Bray I and Fursa D V 1997 *J. Phys. B: At. Mol. Opt. Phys.* **30** 1309–22
- Röder J, Ehrhardt H, Bray I, Fursa D V and McCarthy I E 1996a *J. Phys. B: At. Mol. Opt. Phys.* **29** 2103–14
- Röder J, Ehrhardt H, Bray I, Fursa D V and McCarthy I E 1996b *J. Phys. B: At. Mol. Opt. Phys.* **29** L67–73
- Rösel T, Röder J, Frost L, Jung K and Ehrhardt H 1992 *J. Phys. B: At. Mol. Opt. Phys.* **25** 3859–72
- Scott M P, Stitt T, Scott N S and Burke P G 2002 *J. Phys. B: At. Mol. Opt. Phys.* **35** L323–9
- Shah M B, Elliot D S, McCallion P and Gilbody H B 1988 *J. Phys. B: At. Mol. Opt. Phys.* **21** 2751–61